Exploration workflow for real-time modelling of rock property and AVO feasibilities in areas with complex burial history — a Barents Sea demonstration

Per Avseth[1*], Ivan Lehocki[1], Laurent Feuilleaubois[2], Tore Nordtømme Hansen[1], Kristian Angard[1] and Cyrille Reiser[2]
describe an integrated workflow where full waveform inversion velocity data, well log data, seismic stratigraphy, basin analysis, and rock physics modelling are combined to produce 3D feasibility cubes of expected rock properties and AVO signatures for a given geological scenario. They show how these AVO feasibility cubes can be updated in real time and used to guide quantitative interpretation studies, and to run sensitivity analysis to derisk potential prospects.

Introduction

The petroleum industry is currently experiencing a major paradigm change. A digital transformation is taking place with more automated and integrated workflows and a particular effort to share data and competences in cloud solutions. The remaining reserves of oil and gas are often located in subtle, stratigraphic or combination traps near existing infrastructure, or in structurally complex areas away from well control, where traditional workflows have been insufficient to properly derisk upside potential. These traps will be the future focus for many petroleum companies. A major challenge will be to fast-track oil and gas production from subtle and complex traps more efficiently than before. Integration and automation are key aspects in this process.

Quantitative interpretation will be essential in the hunt for new prospects away from existing wells (Figure 1). It is also important for oil companies to be able to perform fast, yet reliable feasibility studies of expected AVO signatures to maximize the return on purchasing or acquiring prestack seismic data for prospect derisking. In a mature area with good well control, a feasibility study can be conducted using empirical relations derived from local well log data (i.e., near field exploration/ appraisal, see Avseth et al. 2020a). However, in a more frontier setting and/or in areas with limited well control, there is a need to use integrated models that honour local geology (Avseth et al., 2003; Brevik et al., 2011; Dræge et al., 2014; Avseth and Lehocki, 2016; Feuilleaubois et al., 2017a; Lehocki et al., 2020). Rock physics combined with stratigraphic interpretation and thermal modelling can be used to improve the understanding of expected seismic signatures in more frontier settings with limited well control (AlKawai et al., 2018).

In order to accurately model the current rock physics properties of a reservoir, it is key to account for its past burial history. Any differential subsidence, uplift, or heat flow within an area of interest can lead to dramatic lateral changes in reservoir quality

and bias the derisking process. This study is an extension of the workflow introduced by Avseth et al. (2020b) where rock physics combined with burial history is used to create AVO feasibility maps away from well control. First, combined rock physics and compaction modelling (Avseth et al., 2008; Avseth and Lehocki, 2016) is integrated with Full Waveform Inversion (FWI) P-wave seismic velocities and basin analysis to create regional uplift and maximum burial maps for selected horizons/intervals. This allows for the generation of geologically consistent 3D AVO feasibility cubes from (these) maximum burial and net erosion maps,
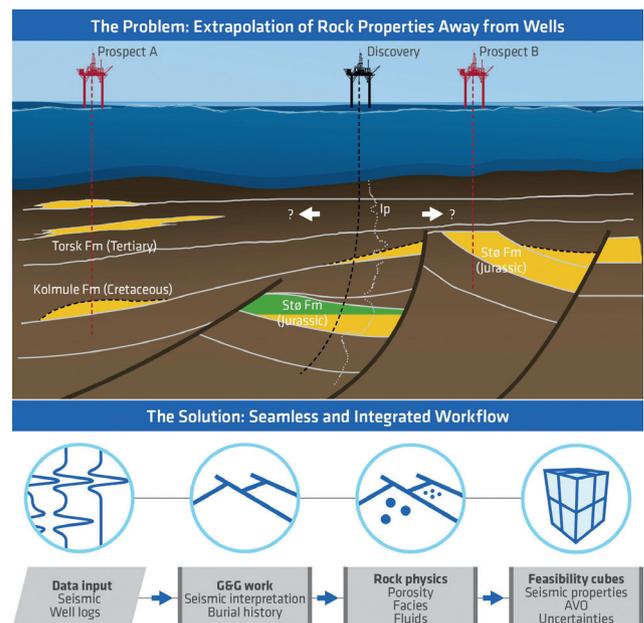
Figure 1 The geologic extrapolation problem. In areas with few wells and complex geology, it is challenging to predict reservoir quality in surrounding prospects away from well control. In this study, we extend on the workflow established by Avseth et al. (2020b), with FWI velocities as input to constrain burial history in an area without well control.

[1] Dig Science | [2] PGS
* Corresponding author, E-mail: Per.Avseth@digscience.no

while also honouring key uncertainties (rock texture, mineralogy, heterogeneity, anisotropy, temperature, etc.). The feasibility cubes can be used to quickly locate prospective areas or directly for lead identification and prospect derisking. Furthermore, they can be used as a fundament to create augmented, non-stationary training data for AVO classification and seismic reservoir prediction in areas with poor well control (c.f. Lehocki et al., 2020). The focus of this paper will be on the novelties in the proposed workflow, including the use of FWI data to create high-resolution uplift (net erosion) maps, the generation of 3D rock property and AVO feasibility cubes, and a demonstration on how to utilize these cubes in QI studies. The technology is demonstrated on data from the Barents Sea, and examples from two prospective targets are shown, one in Paleocene/Eocene deep-marine sands where combined stratigraphic-structural traps are likely to occur, and one in Jurassic shallow marine sands where traps are confined by structural fault-blocks with four-way closure.

Generating uplift maps from FWI velocities and shale trends

The area of study (Harstad-Tromsø basins, West Barents Sea) has been exposed to repeated episodes of rifting, subsidence, uplift, and local salt tectonics. Tectonic uplift and associated net erosion can be estimated from velocity-depth trends (e.g., Japsen, 1999; Hjelstuen et al., 1996, Baig et al., 2017). Based on a reference trend for a given shale interval, representing normal compaction, the deviation from this reference trend can be used to estimate the net uplift. This exercise can be done on well log data and/or on seismic velocity data. Furthermore, the uplifts from velocities should be calibrated/

validated with uplift estimates from other sources of information (e.g., vitrinite reflectance data, sediment mass balance, sandstone diagenesis, apatite fission track analysis, etc.). Johansen (2016) and Avseth et al., (2020b) used seismic stacking velocities for shaly intervals to derive regional uplift maps. In this study, this is extended to high-resolution refraction FWI velocities (Sakariassen et al, 2018; Rønholt et al., 2015), see Figure 2.

Uplift estimates for three key intervals in the area of interest are performed: i) The Torsk Fm interval of Paleocene-Oligocene age, ii) the Cretaceous shales (mainly Kolje and Kolmule Fm), and iii) the Upper Jurassic shales (Hekkingen and Fuglen Fm). This is to account for the possibility of different intervals with different net erosions, due to complex tectonics, and some intervals can be characterized by different types of shales with distinct depth trends. Multiple rift events have occurred in the area (Faleide et al., 2015). These include a major event in the Late Middle Jurassic to Early Cretaceous ages with a northeast-southwest rift axis (when the Tromsø and Harstad basins were developed). Another event in the Late Cretaceous to Paleocene ages with a rift-shear interaction zone represents the opening of the Northern Atlantic between Norway and Greenland (Baig et al., 2017). In both these rift phases, there are local as well as regional tectonic movements that have affected the stratigraphic relationships and sequence boundaries, making it difficult to fully capture the burial history. However, from a rock physics point of view, the key focus is to know the maximum burial depth of the different intervals. This will enable us to quantify to reliably quantify the amount of diagenetic quartz cement that has been generated during burial and uplift. The timing of the tectonic movements is uncertain, but likely maximum burial dates to the Oligocene-Miocene time (Japsen, 1999; Zattin et al, 2017). The uplift estimate map for the Torsk Fm, derived from the FWI velocity cube, seismic horizons, and reference shale trend, is shown in Figure 2.

Burial constrained rock physics modelling and generation of AVO feasibility cubes

Next, forward modelling of the expected rock physics properties and associated AVO responses for selected scenarios is performed, given the input burial history (Figure 3). The methodology introduced by Avseth and Lehocki (2016) for combined compaction and rock physics modelling in 1D is extended, as is the work by Avseth et al. (2020b) on the generation of rock physics and AVO feasibility maps in 2D, to perform full 3D modelling of rock physics properties and associated AVO feasibility cubes. In this way, the expected rock physics properties of a given rock can be predicted, sandstone or shale, at any given location of a 3D cube, while honouring the burial (and thermal) history of the rock at this very location.

The methodology introduced by Avseth and Lehocki (2016) combines rock physics contact theory with diagenetic modelling. For the mechanical compaction domain, porosity versus depth is determined from empirical depth trends (e.g. Ramm and Bjørlykke, 1994). The associated seismic velocities versus depth are determined from Hertz-Mindlin/Walton contact theory (Mavko et al., 2020), and will vary both as a function of porosity and effective stress; the latter can be determined from integration of overburden densities. For the chemical compaction domain,
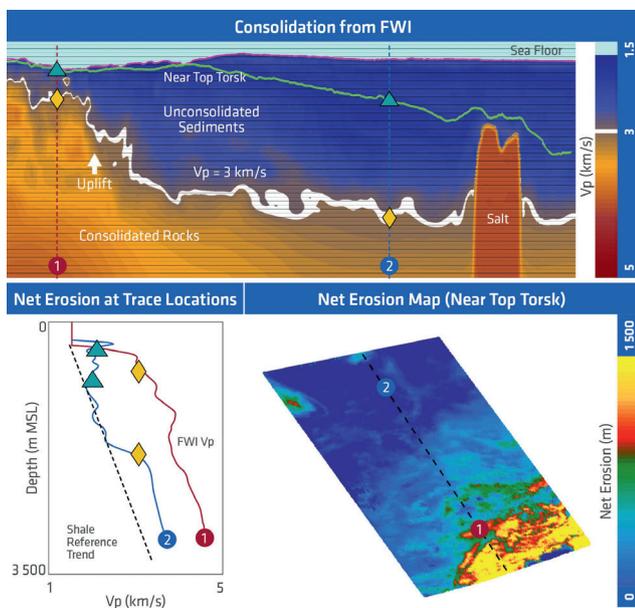
Figure 2 FWI data (upper) along a selected seismic line, and the principles of estimating uplift using normal compaction reference depth trends for shales (displayed for two traces; lower left). To the right, local uplift (net erosion) map for the Torsk Fm, derived from the FWI velocities within a 100 m interval beneath the Near Top Torsk horizon (dashed line indicates section location). The green triangle indicates the depth of the Near Top Torsk Fm and the yellow diamond marks the change from mechanical to chemical compaction occurring around at 3 km/s. The map is showing close to zero uplift in the north-west (basinward) and significant uplift (1000-1500 m) in the south-east (landward). The uplift information is used to constrain the AVO feasibility modelling.
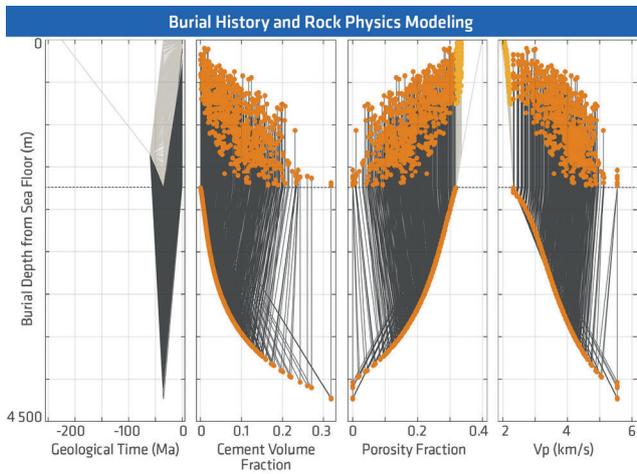
Figure 3 Combined compaction and rock physics modelling of expected rock physics properties at any given location at the Top Stø Fm (capped by Fuglen Fm shale) as a function of burial depth through geological times. The burial history (leftmost subplot) is constrained in the 3D space by uplift derived from FWI velocities as a function of burial depth in metres (BD). From the burial and temperature history, the cement volumes at any location of Top Stø Fm is estimated using the Walderhaug model (1996, second subplot from the left). Porosity-depth trends are updated accordingly (third subplot from the left). Finally, the rock physics properties are estimated at any location, constrained by the burial history and diagenetic evolution (e.g. P-wave velocities shown in rightmost subplot). The black dotted horizontal lines around 1750 m in all subplots indicate the burial depth corresponding to a temperature of 70°C at which quartz cementation initiates (sea-floor temperature = 4°C, temperature gradient = 38°C/km). Note that the orange end-points indicate present-day rock properties, whereas the deepest orange points indicate the rock properties at maximum burial.

the porosities will be affected by quartz cementation that can be quantified from time and temperature using the Walderhaug kinetic model (Walderhaug, 1996), while the Dvorkin-Nur contact cement theory combined with Hashin-Shtrikman is used to model the corresponding seismic velocities (Avseth et al., 2005).

Target reservoir zones are located in the intra-Torsk interval (Paleocene sands), likely to be deposited in the basinal areas, and in Jurassic pre-rift Stø Fm sandstones located in more proximal structurally tilted fault-blocks. Figure 3 shows the result of the combined compaction and rock physics modelling for any given point along the Top Stø Fm horizon in the area of interest. The

orange points show the present depth (uppermost end-points) and the maximum burial depth (lowermost turning-points) at any given spatial location along Top Stø Fm.

A corresponding shale cube is generated from empirical shale depth trends extracted from nearby wells, corrected for net uplift, as shales are abundant in the area. Combining the elastic properties of the sandstone and shale cubes generates so-called AVO feasibility cubes (in 3D) that predict the expected AVO response for a given pore fluid, at any location in the cube.

The resulting feasibility maps in Figure 4 show the modelled reservoir and rock properties along the Top Stø (zoomed into a target area with prospective fault-blocks), and the corresponding AVO feasibility maps, for a given geological scenario. This is the most likely scenario, where the Stø sandstones are assumed to be relatively clean (volume of clay = 0.1), and with medium grain size (0.3 mm), and zero clay coating. Furthermore, the temperature gradient is assumed to be 38°C/km, in agreement with observations from nearby wells. Note that the rock-property and AVO feasibility maps are constrained by the estimated uplifts from the FWI velocities. Hence, local geology is honoured, and there is geological information in these AVO feasibility maps derived from the FWI data. These results are similar to what was obtained by Avseth et al., (2020b) in another area of the Barents Sea, but here the maps show more details as high-resolution FWI velocities are used instead of interval velocities derived from coarse gridded stacking velocities.

Figure 4 clearly shows that the Stø Fm in fault block structures in the area of interest are expected to be poorly consolidated (i.e. approaching zero cement volume on the crest). The reservoir shows significant fluid sensitivities and strong AVO anomalies when saturated with hydrocarbons. There will likely be a change in the AVO class from class 1-2p for a brine saturated reservoir to class 3 when saturated with relatively light oil (30° API) or gas.

Figure 5 shows a 3D AVO feasibility cube and associated rock properties, and focuses on another key target interval, the intra Torsk Fm sandstones of Paleocene/Eocene age. These sands are located more basinward, presently deeper buried than most of the Jurassic Stø Fm, but with significantly smaller or no uplift. As Figure 5 shows, no quartz cementation is expected in these sands
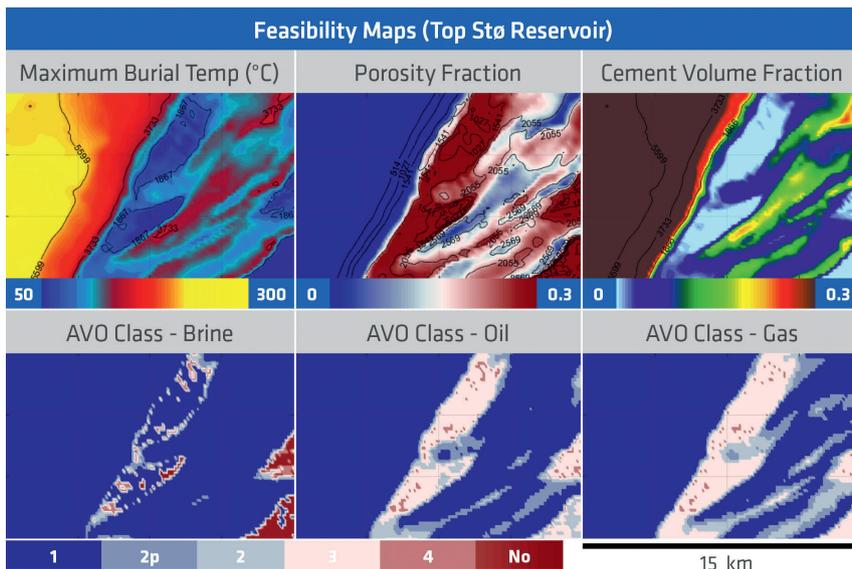
Figure 4 Rock property and AVO feasibility maps in a zoomed-in area focusing on Upper Jurassic fault blocks where Stø Fm is the target reservoir. Contours in upper left subplot are that of maximum burial, upper middle of uplift, and upper right of burial depth, all units being in metres.
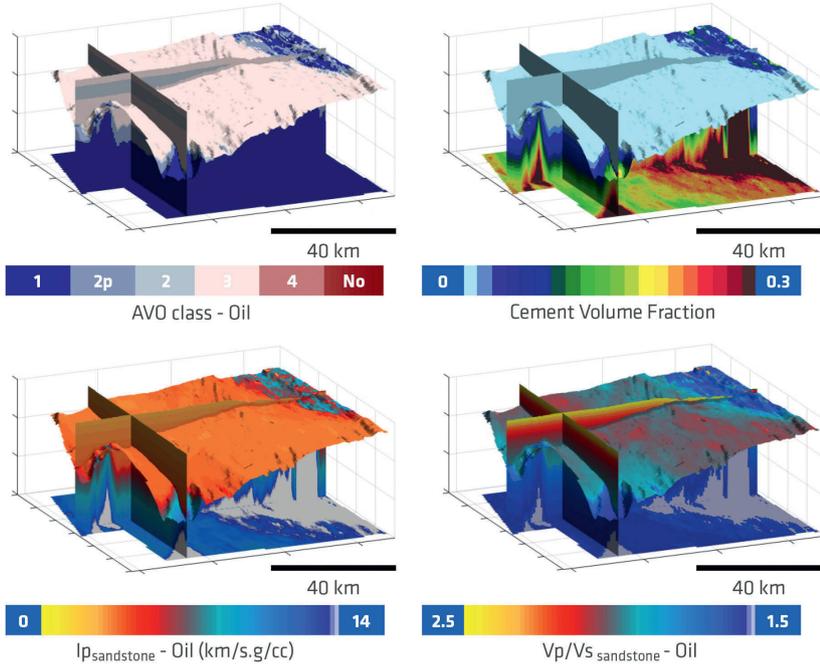
Figure 5 Rock property and AVO feasibility cubes in the area of interest, where Near Top Torsk horizon + 200 m (where target intra Torsk sands are expected) is displayed together with horizontal and vertical intersections. Oil-filled Torsk Fm shows mostly a class 3 AVO response in the area, and cement volume will always be 0, as the sands are not buried deep enough to be cemented.

towards the top of the formation, based on the modelling. This is because the sands have never reached a depth where temperatures are high enough (greater than circa 70°C) to form quartz cement. However, the mechanical compaction must be addressed, with porosity reduction and increasing effective stress with depth. The shale depth trends used for the AVO feasibilities in the Torsk Fm interval, are empirical trends derived from intra Torsk shales in nearby wells. Mainly AVO class 3 for oil-filled Torsk Fm sands is expected, whereas brine sands (not shown here) will cause a class 1 anomaly.

Real-time AVO feasibility modelling for quantitative interpretation of prestack seismic data and sensitivity analysis

Rock property and AVO feasibility cubes can be investigated for expected AVO signatures at any given location of a seismic cube. Geological scenarios and uncertainties in input parameters can be tested in real time and the resulting simulated cubes can be compared with real data in the impedance or reflectivity domains. In this way, the approach enables simultaneous sensitivity analysis and screening of potential fluid related anomalies in prestack seismic data, and more efficient derisking of pre-defined prospects.

An absolute simultaneous prestack seismic inversion was conducted using seismic data acquired with a broadband multisensor towed streamer system. This dataset had been depth migrated using refraction FWI velocities with frequencies up to 12 Hz. The frequency range for the input seismic data to the inversion workflow were from 4 Hz to 50 Hz. The low frequency model was built using the FWI velocity cube and the transformation to the acoustic impedance and velocity ratio was done using a rock physics relationship for shales. Thus, the absolute seismic inversion was generated without the active use of any well control (Feuilleaubois et al., 2017b).

A good match is observed on Figure 6 between the inversion results and the rock physics modelling prediction in the lower Torsk Fm in an area where 600 m of uplift was estimated from the FWI velocities. Accounting for uplift indicates that the transition between mechanical and chemical compaction will be observed locally at a present depth of 1400 m. A hydrocarbon-filled sandstone (most likely in a liquid phase) within this transition zone is suggested by both low acoustic impedance and velocity ratio signatures. Figure 7 shows a 3D view of the geobody corresponding to the lead observed in Figure 6. As observed in 1D, the target depth just entered the cementation window before
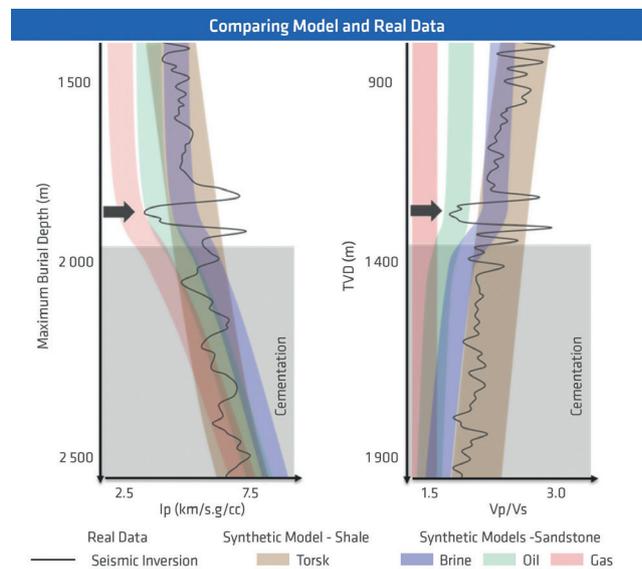
Figure 6 1D trace extraction of absolute acoustic impedance (Ip) and velocity ratio (Vp/Vs) inversion results overlaying the corresponding shale and sandstone rock physics models accounting for an uplift of 600 m in the lower Torsk formation. The black arrow shows a 50 m interval with the Ip and Vp/Vs responses classified as an oil-bearing sandstone.
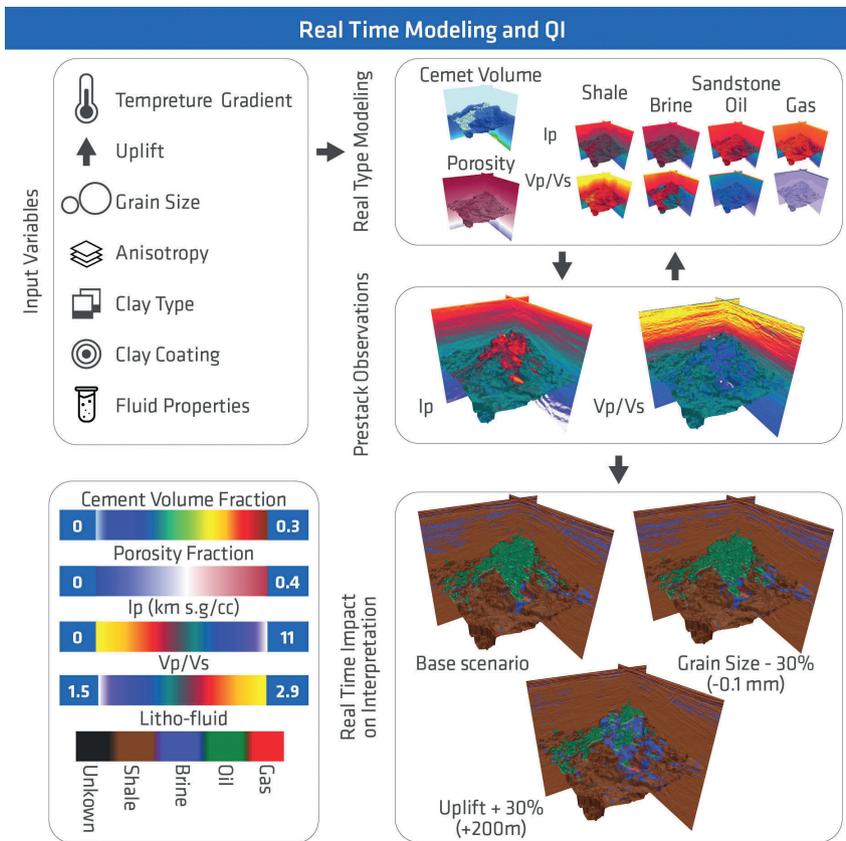
Figure 7 Sensitivity analysis for lithology and fluid derisking in 3D using real time rock physics modelling to test geological scenarios and measure the impact on the quantitative interpretation of broadband prestack seismic data observations.

exhumation, and a porosity of 34% is predicted in the reservoir. Running a sensitivity analysis on hydrocarbons detection in real time, varying input parameters such as grain size or uplift uncertainty, allows an assessment of the uncertainty in the output rock property and AVO feasibility results. While an uncertainty of 30% on the grain size does not lead to a very different outcome, a 30% uncertainty on the uplift will have a significant impact on potential reserves as observed on Figure 7. Knowing such information, an exploration team might want to spend some extra time derisking this lead to reduce the uncertainty of the uplift. Despite a significant impact on the potential reserves, presence of hydrocarbons in this lead remains supported by the comparison of the AVO feasibility cubes and the prestack seismic observations. Scenario-based modelling can be run also by varying input parameters such as: temperature gradient, fluid properties, shale type, clay coating, anisotropy, etc.

The AVO feasibility cubes can furthermore be used to generate and augment training data away from well control during statistical and/or machine learning classification of facies and fluids from seismic amplitude data. The latter is beyond the scope of this study, but will be the focus of future research.

Conclusions

We have demonstrated a novel integrated and seamless workflow for the generation of rock properties and AVO feasibility cubes, with the use of FWI velocity data from the Barents Sea. The methodology enables geologically constrained and robust real-time prediction of expected rock physics properties away from well control in the 3D space. This approach is constrained by high-resolution seismic velocity information (allowing high resolution estimation of uplift at various stratigraphic levels), geological inputs (basin modelling, seismic stratigraphy and facies maps) and rock physics depth trend analysis. The proposed workflow allows for efficient and geologically consistent DHI derisking of leads and prospects in any geological context. More specifically, it allows the interpreter to account for and analyse the impact of geological processes on the final geophysical interpretation by running sensitivity analysis of key input parameters in real time. Such a workflow can support complex prospect risking procedures and the estimation of risked volumes of hydrocarbon. This can provide an integrated organization-wide consistent approach to the DHI-modified risking process used by many companies.

Acknowledgements

References

AlKawi, W., Mukerji, T., Scheirer, A.H., and Graham, S.A. [2018]. Combining seismic reservoir characterization workflows with basin modeling in the deepwater Gulf of Mexico Mississippi Canyon area. *AAPG Bulletin*, **102**, 629-652.

Avseth, P., Flesche, H., and van Wijngaarden, A-J. [2003]. AVO classification of lithology and pore fluids constrained by rock physics depth trends. *The Leading Edge*, **22**, 1004-1011.

Avseth, P., Mukerji, T., and Mavko, G. [2005]. *Quantitative Seismic Interpretation – Applying Rock Physics Tools to Reduce Interpretation Risk*. Cambridge University Press.

Avseth, P., Dræge, A., van Wijngaarden A-J., Johansen, T., and Jørstad, A. [2008]. Shale rock physics and implications for AVO analysis: A North Sea demonstration. *The Leading Edge*, **27**, 697–824.

Avseth, P., and Lehocki, I. [2016]. Combining burial history and rock-physics modeling to constrain AVO analysis during exploration. *The Leading Edge*, **35**, 528-534.

Avseth, P., Lehocki, I., Kjøsnes, Ø., and Sandstad, O. [2020a]. Data-Driven Rock Physics Analysis of North Sea Tertiary Reservoir Sands. *Geophysical Prospecting,* in press.

Avseth, P., Lehocki, I., Angard, K., Hansen, T., Shelavina, E., and Schjelderup, S. [2020b]. A new integrated workflow to generate AVO feasibility maps for prospect de-risking. *EAGE Annual Conference and Exhibition,* Extended Abstract.

Baig, I., Faleide, J.E., Jahren, J., and Mondol, N. [2016]. Cenozoic exhumation on the southwestern Barents Shelf: Estimates and uncertainties constrained from compaction and thermal maturity analyses. *Marine and Petroleum Geology*, **73**, 105-130.

Brevik, I., Callejon, A., Kahn, P., Janak, P., and Ebrom, D. [2011]. Rock physicists step out of the well location, meet geophysicists and geologists to add value in exploration analysis. *The Leading Edge*, **30**, 1382-1391.

Dræge, A., Duffaut, K., Wiik, T., and Hokstad, K. [2014]. Linking rock physics and basin history — Filling gaps between wells in frontier basins. *The Leading Edge*, **33**, 240-246.

Faleide, J.I., Bjørlykke, K. and Gabrielsen, R.H. [2015], Geology of the Norwegian continental shelf. K. Bjørlykke (Ed.), *Petroleum Geoscience – From Sedimentary Environments to Rock Physics* (2nd edition), Springer-Verlag, 603-637.

Feuilleaubois, L. O., Maioli, A., and Reiser, C. [2017a]. Triassic Regional Rock Physics Study in the Eastern Barents Sea for Prospectivity Analysis. *EAGE*, Extended Abstract.

Feuilleaubois, L.O., Charoing, V., Maioli, A, and Reiser, C. [2017b]. Utilizing a novel quantitative interpretation workflow to derisk shallow hydrocarbon prospects – a Barents Sea case study. *First Break*, **35**, 85-98.

Hjelstuen, B.O., Elverhøi, A., and Faleide, J.I. [1996]. Cenozoic erosion and sediment yield in the drainage area of the Storfjorden Fan. In Solheim, A.,Riis, F., Elverhoi, A., Faleide, J.I., Jensen, L.N., and Cloetingh, S. (Eds.), *Impact of Glaciations on Basin Evolution: Data and Models from the Norwegian Margin and Adjacent Areas*. Global Planet. Change, 12:95–117.

Japsen, P. [1999]. Overpressured Cenozoic shale mapped from velocity anomalies relative to a baseline for marine shale, North Sea. *Petroleum Geoscience*, **5**, 321-336.

Johansen, N. [2016]. *Regional net erosion estimations and implications for seismic AVO signatures in the western Barents Sea.* Unpublished Master Thesis, NTNU, Trondheim, Norway.

Lehocki, I., Avseth, P. and Mondol, N. [2020]. Seismic methods for fluid discrimination in areas with complex geological history-a case example from the Barents Sea. *Interpretation*, Accepted for publication.

Mavko, G., Mukerji, T. and Dvorkin, J. [2020]. *The Rock Physics Handbook*, 3rd edition, Cambridge University Press.

Ramm, M. and Bjørlykke, K. [1994]. Porosity/depth trends in reservoir sandstones: assessing the quantitative effects of varying pore-pressure, temperature history and mineralogy, Norwegian Shelf data. Clay Minerals, **29**, 475-490.

Rønholt, G., Korsmo, Ø., Naumann, S., Marinets, S., Brenne, E., and Abbasi, M., F. [2015] Complete wavefield imaging for lithology and fluid prediction in the Barents Sea Grunde. *SEG Annual Meeting*, Expanded Abstracts.

Sakariassen, R., O'Dowd, N., Naumann, S. [2018]. Barents Sea – A First Look at New High Resolution 3D Multicomponent Seismic. *GeoExpro*, **15** (6), 28-32.

Walderhaug, O. [1996]. Kinetic Modelling of Quartz Cementation and Porosity Loss in Deeply Buried Sandstone Reservoirs. *AAPG Bulletin*, **80**, 731-745.

Zattin, M., Andreucci, B., de Toffoli, B., Grigo, D., and Tsikalas, F. [2016]. Thermochronological constraints to late Cenozoic exhumation of the Barents Sea Shelf. *Marine and Petroleum Geology*, **73**, 97-104.